



NEGATIVE REFRACTION IN RARE-EARTH DOPED CRYSTALS

Deniz Yavuz
UNIVERSITY OF WISCONSIN SYSTEM MADISON WI

06/09/2016
Final Report

DISTRIBUTION A: Distribution approved for public release.

Air Force Research Laboratory
AF Office Of Scientific Research (AFOSR)/ RTB1
Arlington, Virginia 22203
Air Force Materiel Command

DISTRIBUTION A: Distribution approved for public release.

REPORT DOCUMENTATION PAGE					Form Approved OMB No. 0704-0188	
<p>The public reporting burden for this collection of information is estimated to average 1 hour per response, including the time for reviewing instructions, searching existing data sources, gathering and maintaining the data needed, and completing and reviewing the collection of information. Send comments regarding this burden estimate or any other aspect of this collection of information, including suggestions for reducing the burden, to the Department of Defense, Executive Service Directorate (0704-0188). Respondents should be aware that notwithstanding any other provision of law, no person shall be subject to any penalty for failing to comply with a collection of information if it does not display a currently valid OMB control number.</p> <p>PLEASE DO NOT RETURN YOUR FORM TO THE ABOVE ORGANIZATION.</p>						
1. REPORT DATE (DD-MM-YYYY) 27-5-2016		2. REPORT TYPE Final Performance Report			3. DATES COVERED (From - To) March 2013-February 2016	
4. TITLE AND SUBTITLE NEGATIVE REFRACTION IN RARE-EARTH DOPED CRYSTALS				5a. CONTRACT NUMBER FA9550-13-1-0111		
				5b. GRANT NUMBER		
				5c. PROGRAM ELEMENT NUMBER		
6. AUTHOR(S) Yavuz, Deniz D. Brewer, Nick R. Buckholtz, Zach Simmons, Zach J.				5d. PROJECT NUMBER		
				5e. TASK NUMBER		
				5f. WORK UNIT NUMBER		
7. PERFORMING ORGANIZATION NAME(S) AND ADDRESS(ES) University of Wisconsin-Madison Department of Physics 1150 University Avenue, Madison, WI, 53705					8. PERFORMING ORGANIZATION REPORT NUMBER	
9. SPONSORING/MONITORING AGENCY NAME(S) AND ADDRESS(ES) Air Force Office of Scientific Research 875 North Randolph Street Suite 325, Room 3112 Arlington VA, 22203					10. SPONSOR/MONITOR'S ACRONYM(S) AFOSR	
					11. SPONSOR/MONITOR'S REPORT NUMBER(S)	
12. DISTRIBUTION/AVAILABILITY STATEMENT Distribution A- Approved for public release						
13. SUPPLEMENTARY NOTES						
14. ABSTRACT In this project, our long-term goal is to demonstrate the first negative refraction in atomic systems. Although the concept of negative refraction remained an academic curiosity for a long time, it is now well-understood that negative refraction may have important and far-reaching practical implications. The key challenge in observing negative refraction in the optical region of the spectrum is the weakness of the magnetic response. Our central experimental result during this project has been the first observation of Rabi flopping of a magnetic dipole transition in the optical region of the spectrum. We have performed this experiment using the 7F0-5D1 transition of europium ions in a cryogenically cooled doped crystal. This is a major result; we have shown for the first time that an electron can interact sufficiently strongly with the magnetic field of a light wave and coherently move between the levels. Another important result during this project was the proposal for a new type of materials that exhibit negative refraction. Because of these achievements, observing negative refraction and left-handed electromagnetic waves in atomic systems seem within reach for the first time.						
15. SUBJECT TERMS						
16. SECURITY CLASSIFICATION OF:			17. LIMITATION OF ABSTRACT UU	18. NUMBER OF PAGES 14	19a. NAME OF RESPONSIBLE PERSON Prof. Deniz D. Yavuz	
a. REPORT	b. ABSTRACT	c. THIS PAGE			19b. TELEPHONE NUMBER (Include area code) 608-263-9399	

INSTRUCTIONS FOR COMPLETING SF 298

1. REPORT DATE. Full publication date, including day, month, if available. Must cite at least the year and be Year 2000 compliant, e.g. 30-06-1998; xx-06-1998; xx-xx-1998.

2. REPORT TYPE. State the type of report, such as final, technical, interim, memorandum, master's thesis, progress, quarterly, research, special, group study, etc.

3. DATES COVERED. Indicate the time during which the work was performed and the report was written, e.g., Jun 1997 - Jun 1998; 1-10 Jun 1996; May - Nov 1998; Nov 1998.

4. TITLE. Enter title and subtitle with volume number and part number, if applicable. On classified documents, enter the title classification in parentheses.

5a. CONTRACT NUMBER. Enter all contract numbers as they appear in the report, e.g. F33615-86-C-5169.

5b. GRANT NUMBER. Enter all grant numbers as they appear in the report, e.g. AFOSR-82-1234.

5c. PROGRAM ELEMENT NUMBER. Enter all program element numbers as they appear in the report, e.g. 61101A.

5d. PROJECT NUMBER. Enter all project numbers as they appear in the report, e.g. 1F665702D1257; ILIR.

5e. TASK NUMBER. Enter all task numbers as they appear in the report, e.g. 05; RF0330201; T4112.

5f. WORK UNIT NUMBER. Enter all work unit numbers as they appear in the report, e.g. 001; AFAPL30480105.

6. AUTHOR(S). Enter name(s) of person(s) responsible for writing the report, performing the research, or credited with the content of the report. The form of entry is the last name, first name, middle initial, and additional qualifiers separated by commas, e.g. Smith, Richard, J, Jr.

7. PERFORMING ORGANIZATION NAME(S) AND ADDRESS(ES). Self-explanatory.

8. PERFORMING ORGANIZATION REPORT NUMBER.

Enter all unique alphanumeric report numbers assigned by the performing organization, e.g. BRL-1234; AFWL-TR-85-4017-Vol-21-PT-2.

9. SPONSORING/MONITORING AGENCY NAME(S) AND ADDRESS(ES). Enter the name and address of the organization(s) financially responsible for and monitoring the work.

10. SPONSOR/MONITOR'S ACRONYM(S). Enter, if available, e.g. BRL, ARDEC, NADC.

11. SPONSOR/MONITOR'S REPORT NUMBER(S). Enter report number as assigned by the sponsoring/monitoring agency, if available, e.g. BRL-TR-829; -215.

12. DISTRIBUTION/AVAILABILITY STATEMENT. Use agency-mandated availability statements to indicate the public availability or distribution limitations of the report. If additional limitations/ restrictions or special markings are indicated, follow agency authorization procedures, e.g. RD/FRD, PROPIN, ITAR, etc. Include copyright information.

13. SUPPLEMENTARY NOTES. Enter information not included elsewhere such as: prepared in cooperation with; translation of; report supersedes; old edition number, etc.

14. ABSTRACT. A brief (approximately 200 words) factual summary of the most significant information.

15. SUBJECT TERMS. Key words or phrases identifying major concepts in the report.

16. SECURITY CLASSIFICATION. Enter security classification in accordance with security classification regulations, e.g. U, C, S, etc. If this form contains classified information, stamp classification level on the top and bottom of this page.

17. LIMITATION OF ABSTRACT. This block must be completed to assign a distribution limitation to the abstract. Enter UU (Unclassified Unlimited) or SAR (Same as Report). An entry in this block is necessary if the abstract is to be limited.

AFOSR Final Performance Report

Grant/Contract Title: NEGATIVE REFRACTION IN RARE-EARTH
DOPED CRYSTALS **Grant/Contract Number:** FA9550-13-1-0111

Program Manager: Tatjana Curcic

Principal Investigator: Deniz D. Yavuz

1 Abstract and summary of accomplishments

In this project, our long-term goal is to demonstrate the first negative refraction in atomic systems. Although the concept of negative refraction remained an academic curiosity for a long time, it is now well-understood that negative refraction may have important and far-reaching practical implications. About a decade ago it was discovered that negative index materials can be used to construct devices that can image objects with, in principle, unlimited resolution, i.e., perfect lenses. Currently, many groups around the world are working towards constructing high-quality negative index materials with low absorption. Whereas most groups with this goal rely on meta-materials (artificially constructed structures), we are using atomic systems that are driven with lasers in their internal states.

The key challenge in observing negative refraction in the optical region of the spectrum is the weakness of the magnetic response. Our central experimental result during this project has been the first observation of Rabi flopping of a magnetic-dipole transition in the optical region of the spectrum. We have performed this experiment using the ${}^7F_0 \rightarrow {}^5D_1$ transition of europium ions in a doped yttrium orthosilicate ($\text{Eu}^{+3}:\text{Y}_2\text{SiO}_5$) crystal at a temperature of 4 °K. As we will discuss below, we have been able to achieve Rabi flopping frequencies approaching 1 MHz. This is a major result; we have shown for the first time that an electron can interact sufficiently strongly with the magnetic-field of a light wave and move coherently between the two levels (as a result of the magnetic interaction). Another important result during this project was the proposal of a new type of materials that exhibit negative refraction. These are materials where the medium is polarized and magnetized externally, i.e., through means other than the incident probe wave (for example, using other lasers and optical nonlinearities). Compared to materials with a negative refractive index, there is one clear advantage of materials with induced polarization and magnetization: the formation of left-handed waves does not require the stringent material properties (such as the strength of the resonances, the density of radiators, and so on).

2 Background and introduction

Since they were first predicted by Veselago about five decades ago [1], there has been a growing interest in materials with a negative refractive index. Although negative index materials were initially mostly an academic curiosity, it is now well-understood that these materials may have important applications such as constructing lenses that beat the diffraction limit [2], engineering electromagnetic cloaks [3], and transformative optics [4]. Negative index materials do not exist naturally, and thus they need to be artificially constructed. One approach is to engineer periodic metal-dielectric structures, termed meta-materials, with appropriate electric and magnetic resonances. Initial experiments demonstrated negative refractive index in the microwave region of the spectrum using meta-materials constructed from metal wires and split-ring resonators [5, 6]. Inspired by these microwave experiments, utilizing advances in nano-lithography techniques, a number of groups have reported negative refractive index at optical frequencies in metal-dielectric

nano-structures and photonic crystals [7, 8]. Another approach for negative refractive index, which is somewhat complementary to the meta-material approach, is to use atomic systems [9–14]. Here the idea is to use sharp electric-dipole and magnetic-dipole transitions and modify the permittivity and permeability appropriately. In the spirit of electromagnetically induced transparency (EIT) and related techniques [15, 16], the atomic system can be dressed with strong lasers in such a way to produce a negative refractive index for a weak probe laser beam.

Our long-term goal in this project is to experimentally obtain negative refraction with low absorption in the optical region of the spectrum using a driven atomic system. The key advantages of this approach over meta-materials are: (i) atomic systems are uniquely suited for achieving negative refraction at shorter and shorter wavelengths, particularly in the visible and ultraviolet regions of the spectrum, and (ii) since negative refraction is achieved through manipulation of internal states, the optical properties can be dynamically modified, opening an array of exciting applications including perfect-lens switches. Despite these key advantages, achieving negative refraction in atomic systems is a challenging task that has not yet been experimentally demonstrated. In the optical region of the spectrum, the greatest challenge is the weakness of the magnetic response. It is well-known that the magnetic susceptibility is typically smaller than its electric counterpart by a factor of $(\alpha/2)^2 \sim 10^{-5}$, and as a result, it is simply impossible to talk to the magnetic-field of a wave strongly in many atomic systems. As we will discuss in detail below, this challenge can be overcome in rare-earth doped crystals cooled to cryogenic temperatures.

Our key achievements during this project, which we will detail below, can be summarized as follows: (i) We have identified a strong magnetic-dipole transition in europium ions (${}^7F_0 \rightarrow {}^5D_1$ transition), and constructed an experimental system to study this transition in $\text{Eu}^{+3}:\text{Y}_2\text{SiO}_5$ (hereafter abbreviated as Eu:YSO). (ii) We performed the first precision spectroscopy, excited state lifetime, and spectral hole burning studies of this transition. (iii) We have observed Rabi flopping of this transition at a rate approaching 1 MHz. As mentioned above, this is the first time Rabi flopping of a magnetic-dipole transition in the optical region has been observed. (iv) We have proposed a new approach for producing left-handed waves and negative refraction in a medium. In these externally polarized and magnetized materials (hereafter abbreviated as EIPM materials), the formation of left-handed waves does not require as stringent material properties (compared to negative-index materials). (v) We have evaluated this new scheme in Eu:YSO, and our numerical calculations predict that negative refraction can be observed inside an Eu:YSO crystal using modest experimental parameters.

3 Experimental investigations in Eu:YSO

Rare-earth doped crystals at cryogenic temperatures offer a promising route for negative refraction studies. As mentioned above, the chief difficulty for observing these effects in the optical region of the spectrum is the weakness of the magnetic response. This challenge can be overcome using the intra-configurational $4f \rightarrow 4f$ transitions of rare earth ions [17, 18]. Rare earths typically form trivalent ions in crystals with only $4f$ electrons remaining in the outer shell in the ground configuration. The $4f$ shell is tightly bound to the nucleus and the $4f$ electronic configuration interacts weakly with the crystal environment. As a result, the intra-configurational $4f \rightarrow 4f$ transitions are sharp, and they are very much like free-ion transitions that are only weakly perturbed by the crystal field. At cryogenic temperatures, homogeneous linewidths well-below 1 MHz are routinely observed for the $4f \rightarrow 4f$ transitions [17, 19, 22]. Another attractive feature of these systems is that doping fractions of $\sim 0.1\%$ are routinely used, which corresponds to rare-earth ion densities

exceeding $10^{19} / \text{cm}^3$. These densities are much higher than what can be achieved in neutral ultracold clouds or atomic vapors. The rare-earth ion-ion interactions do not significantly affect the $4f$ configuration at these densities. Because of the interaction with the crystal field, there is an inhomogeneous broadening of the intra-configurational $4f \rightarrow 4f$ lines [17, 19]. This broadening depends on the crystal host and the specific levels, but is typically a few GHz (as we will discuss below, we have measured this width to be 4.5 GHz for the ${}^7\text{F}_0 \rightarrow {}^5\text{D}_1$ transition in Eu:YSO). This broadening is unusually small for a solid state system, which is again a result of the $4f$ configuration being relatively well shielded from the crystalline environment. These attractive properties of rare earth doped crystals have been essential in demonstrations of quantum interference effects such as EIT and slow light in these systems [20, 21].

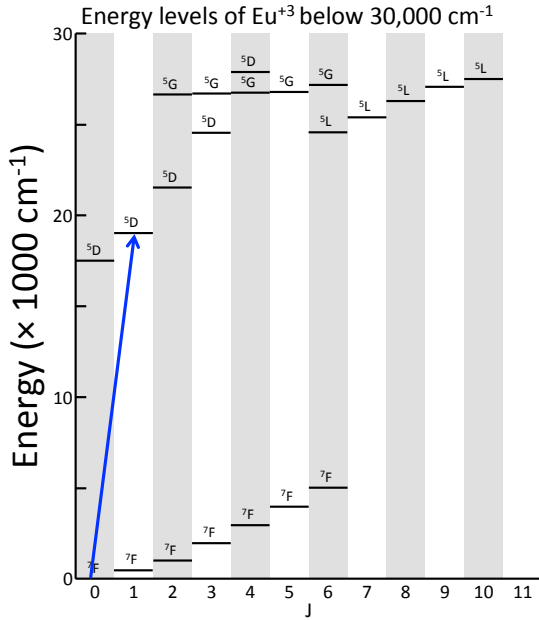


Figure 1: The levels of the Eu^{+3} ions within the $4f^6$ configuration with energies below $30,000 \text{ cm}^{-1}$. We use the ${}^7\text{F}_0 \rightarrow {}^5\text{D}_1$ (shown with an arrow) strong magnetic dipole transition at a wavelength of 527.4 nm. All quantum optics investigations of Eu^{+3} to date have utilized the ${}^7\text{F}_0 \rightarrow {}^5\text{D}_0$ transition at a wavelength of 580 nm.

The Eu:YSO crystal has been studied intensively over the last decade within the context of quantum memories due to its exceptional decoherence properties [17, 22, 23]. These decoherence properties make this crystal very attractive for negative refraction studies. The levels of the Eu^{+3} ions within the $4f^6$ configuration with energies below $30,000 \text{ cm}^{-1}$ are shown in Fig. 1. All quantum optics investigations of Eu^{+3} to date have utilized the ${}^7\text{F}_0 \rightarrow {}^5\text{D}_0$ transition at a wavelength of 580 nm. Very recently, the magnetic-dipole nature of the ${}^7\text{F}_0 \rightarrow {}^5\text{D}_1$ optical transition has been demonstrated using an Eu^{+3} doped nano-particle [24].

Fluorescence studies: Our first task was to precisely measure the transition wavelength of the ${}^7\text{F}_0 \rightarrow {}^5\text{D}_1$ transition. For this purpose, we performed high-resolution fluorescence studies of the crystal using excitation with ultraviolet (UV) light. We excite the crystal using a UV light-emitting diode (LED) array in the wavelength range 360-390 nm. The UV light excites the ions to closely-spaced L, G, and H levels in the $4f$ shell (Fig. 1). The excitation then decays back to the ground F levels through a number of decay channels. We observe ~ 50 fluorescence lines in the wavelength region 500 nm-700 nm. Figure 2 shows the observed fluorescence spectrum of the ${}^7\text{F}_0 \rightarrow {}^5\text{D}_1$ transition near a wavelength of 527 nm. The spectrum is recorded using a 3-m-long high-resolution Echelle grating spectrometer. Different m_J states of the excited level ${}^5\text{D}_1$ are split due to the strong crystal field. We observe fluorescence from the two m_J transitions from each of the two different

sites in the crystal. We decided to use the 527.4 nm transition of site 2 since it has the strongest transition matrix element.

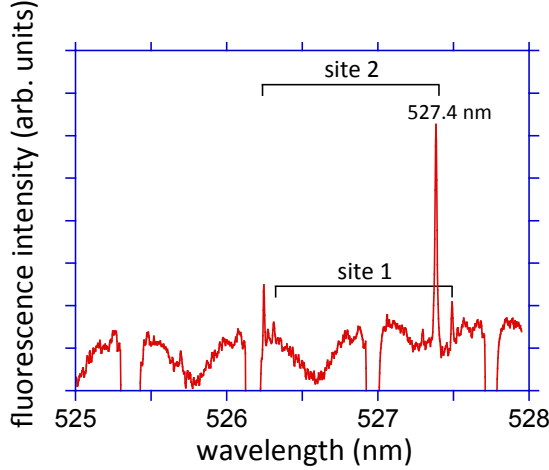


Figure 2: The observed fluorescence spectrum of the ${}^7F_0 \rightarrow {}^5D_1$ of the transition. The spectrum is recorded using a 3-m-long high-resolution Echelle grating spectrometer. We observe fluorescence from the two m_J transitions from each of the two Eu^{+3} sites (site 1 and site 2) in the crystal.

Laser system and experimental setup: Our laser system starts with a custom-built external cavity infrared diode laser at a wavelength of 1054.8 nm. The diode laser produces a continuous-wave (CW) optical power of 20 mW with a free-running frequency linewidth of about 0.5 MHz. We lock the frequency of the diode laser to a high-finesse, ultra-low expansion (ULE) glass cavity, which serves as a frequency reference for the experiment and also reduces the laser linewidth to about 10 kHz. The diode laser output is amplified to 10 W using a ytterbium fiber amplifier. The fiber amplifier output is frequency doubled to a green wavelength of 527.4 nm using intra-cavity second harmonic generation with a KTP crystal. We typically achieve about 30% conversion efficiency from the infrared to green light. The green light produced in the cavity is beam shaped and then passes through acousto-optic modulators for frequency and timing control. The beam is then focused onto a 1-cm-long Eu:YSO crystal, which is housed inside a continuous-flow, liquid-helium cryostat.

Measurement of the lifetime of the 5D_1 level: The homogeneous linewidth of the excited 5D_1 level is an important parameter for our experiment. This linewidth has many contributions including magnetic-dipole decay rate to the ground level, multi-phonon non-radiative decay to the 5D_0 level, and dephasing due to ion-ion and ion-host interactions. A detailed discussion of various decay and dephasing mechanisms of optical transitions in rare-earth doped crystals can be found in Refs. [25, 26]. At cryogenic temperatures, the dominant decay mechanism is the phonon induced non-radiative decay to the level with the nearest energy (5D_0 in this case). We have measured the decay rate of the 5D_1 level using excitation with a short green laser pulse. For this purpose, following laser excitation, we collect the orange fluorescence from the 5D_0 level to the ground F levels as a function of time. As shown in Fig. 3, the fluorescence signal out of the 5D_0 level shows a sharp increase followed by a slow exponential decay. The increase is a result of the phonon-induced decay from the 5D_1 to 5D_0 . The rise-time of this increase is measured to be 30 μs , which is the decay time of the 5D_1 level (i. e. decay rate of 33 kHz). This decay time is remarkably long considering that this is a solid state environment.

Absorption spectroscopy of the ${}^7F_0 \rightarrow {}^5D_1$ transition: Figure 4(a) shows the transmission of a weak (optical power of about 1 μW) green beam through the crystal as its frequency is scanned across the ${}^7F_0 \rightarrow {}^5D_1$ resonance at a crystal temperature of 4° K. We observe a (highly-

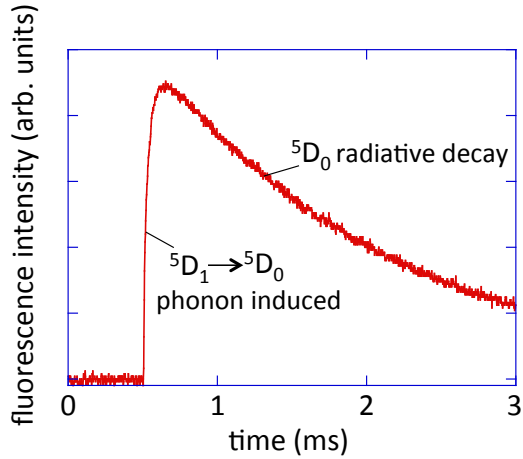


Figure 3: Fluorescence intensity out of the 5D_0 level following excitation of the 5D_1 level with a short green laser pulse. The initial increase with a rise-time of $30 \mu s$ is a result of the phonon-induced decay from 5D_1 to 5D_0 .

saturated) resonance width of about 4.5 GHz, which is similar to the width of the $^7F_0 \rightarrow ^5D_0$ line in recent quantum memory experiments [23]. As mentioned above, the width is determined by the inhomogeneous broadening which is a result of the crystal strains and local variations in the crystal field. The on-resonant absorption that we observe (optical depth) is very good considering that we are probing a magnetic dipole transition. The photograph in Fig. 4(b) shows the orange fluorescence of the crystal due to the absorption of the green light (the laser light is propagating from right to left and the photograph is taken from the side). The green beam's absorption is directly seen since the fluorescence tapers off from right to left.

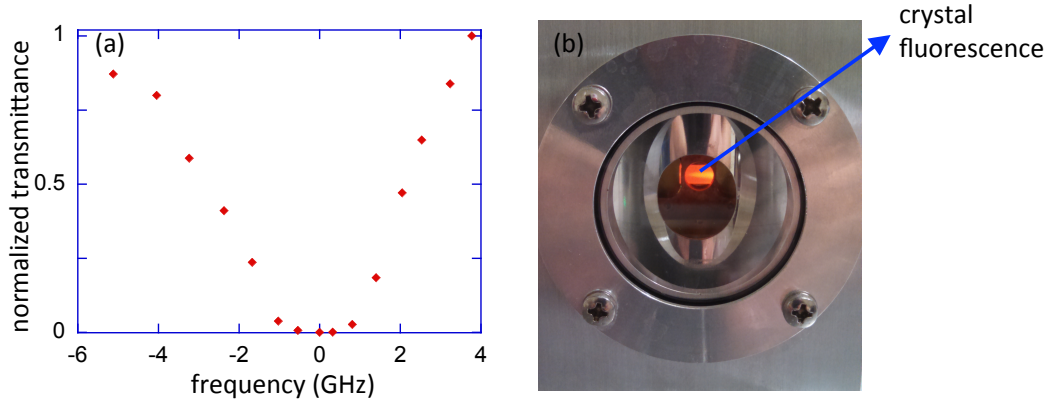


Figure 4: (a) The transmission of the green beam through the crystal as its frequency is scanned across the $^7F_0 \rightarrow ^5D_1$ resonance. We observe a highly-saturated resonance width of about 4.5 GHz and very good on-resonance optical depth. (b) The orange fluorescence of the crystal due to the absorption of the green light. The laser light is propagating from right to left and the photograph is taken from the side. The green beam's absorption is directly seen since the fluorescence tapers off from right to left.

Spectral hole burning: We have also observed spectral hole burning under the broad inhomogeneous profile. For this purpose, we first illuminate the crystal with a reasonably strong pump laser beam (optical power of a few mW) whose frequency is tuned close to the center of the inhomogeneous profile [near “0” in Fig. 4(a)]. The pump beam addresses a select group of atoms and redistributes the populations of the hyperfine levels. We then measure the absorption of a weak probe laser as its frequency is scanned across the resonance. As a result of the spectral hole established by the pump laser, the probe is transmitted through the crystal even though its frequency

is tuned close to the center of the inhomogeneous profile. Figure 5 shows the transmission of the probe laser as its frequency is scanned across the spectral hole. Here, “0” of the horizontal axis is the frequency in which the probe laser frequency coincides with that of the pump laser. We have measured the lifetime of the spectral holes to be quite long, exceeding many minutes. The observed width of the spectral hole (1.8 MHz) is currently limited by the technical limitations of our set-up. Once we overcome a number of technical issues, the width of the spectral holes will be limited by the homogeneous linewidth of the ${}^7F_0 \rightarrow {}^5D_1$ transition. As shown in the measurement of Fig. 3, this linewidth is expected to be at the 30 kHz level.

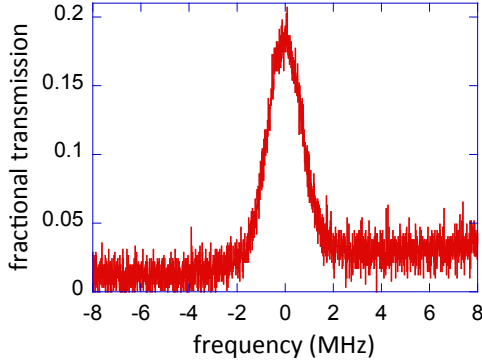


Figure 5: Transmission of the probe laser beam as its frequency is scanned across the spectral hole established by the pump laser beam. We observe a spectral hole width of 1.8 MHz with a peak transmission of about 20%. The lifetimes of the spectral holes are long, exceeding many minutes.

Rabi flopping of the ${}^7F_0 \rightarrow {}^5D_1$ transition: We next proceed with a detailed description of our Rabi flopping experiments. For these experiments, we tune the laser to about the center of the inhomogeneous profile and split the beam into two. One part of the beam has substantial optical power (of order 100 mW) and is focused to a $1/e^2$ intensity radius of $55\ \mu\text{m}$ in the crystal. This beam serves as the Rabi flopping beam. The second part of the beam is very weak (with optical power of less than 1 pW) and it counter-propagates to the Rabi flopping beam. This beam serves as the probe and the transmission of this beam indicates the percentage of the ions that have been excited to the 5D_1 level. The experimental timing cycle is as follows. We start the experiment with all the ions initialized to the ground 7F_0 level. With the ions starting in the ground state, we apply a Rabi flopping pulse of certain duration to the ions. After the Rabi flopping pulse is applied, we turn-on a short probe pulse and measure the transmission of the probe through the crystal with a sensitive photo-detector. The Rabi flopping of the ions is then reflected on the transmission of the probe laser beam. If, for example, the duration of the Rabi beam is chosen such that we have a π pulse, then the atoms would be excited to the 5D_1 level and we would expect reduced absorption (or net gain if inversion is achieved) on the probe laser. If on the other hand we apply a 2π pulse, we would expect atoms to flop back to the ground state, resulting in increased absorption.

Figure 6 shows the transmission of the probe laser beam as the duration of the Rabi pulse is varied. For this measurement, the optical power in the Rabi flopping beam is kept at a constant value of 200 mW. There is a clear Rabi cycle with a Rabi flopping frequency of 770 kHz. As mentioned above, this is the first time Rabi flopping is observed for a magnetic-dipole transition in the optical region of the spectrum. Similar to Rabi flopping experiments of the quantum-memory transition [23], the Rabi oscillation quickly dies out after about one-cycle. In rare-earth doped systems, there are many different contributions to this fast dephasing of the Rabi oscillations. For our experiment, the dominant contribution is the variation of the magnetic dipole matrix element between specific hyperfine transitions. In this experiment, we are not using spectral hole

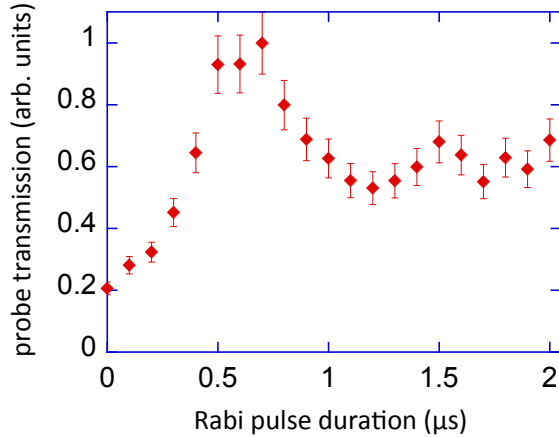


Figure 6: The transmission of the probe laser beam as the duration of the Rabi pulse is varied. We observe Rabi flopping with a frequency of 770 kHz. The Rabi oscillation quickly dies out after about one cycle due to a variety of dephasing processes. For our experiment, the dominant contribution is the variation of the magnetic dipole matrix elements between specific hyperfine transitions.

burning followed by pumping/repumping to select a specific hyperfine transition for a unique class of atoms under the broad inhomogeneous profile. As a result, the Rabi flopping laser simultaneously excites ions using different transitions from the ground level hyperfine manifold to the excited level manifold (there are nine possible such transitions). The variation of the Rabi frequencies of the transitions result in a fast dephasing of the observed Rabi cycle of Fig. 6. We have performed density-matrix numerical simulations of our system including the inhomogeneous broadening and all possible hyperfine transitions. Our preliminary numerical results show dephasing of the Rabi oscillations very similar to the experimental data of Fig. 6.

In Fig. 7, we repeat the Rabi flopping measurement of Fig. 6 at different beam powers. As the beam power is reduced, the Rabi flopping frequency steadily decreases. Figure 8 summarizes the results of the measurements of Fig. 7. As the beam power is varied from 165 mW to 37 mW, the Rabi flopping frequency decreases from 625 kHz to 312 kHz, respectively. The Rabi flopping frequency equals $\Omega = B\mu/\hbar$ where μ is the magnetic-dipole matrix element of the ${}^7F_0 \rightarrow {}^5D_1$ transition and B is the magnetic field of the wave. As a result, we would expect the observed Rabi frequency to be proportional to the square-root of the beam power. The solid line in Fig. 8 shows that the data points fit well to the expected square-root dependence.

The significance of the data of Fig. 8 is that the fit to the data points (solid curve) allows us to extract the value of the magnetic-dipole matrix element. We find this value to be $\langle {}^7F_0, m_J = 0 | \mu_1^{(1)} | {}^5D_1, m_{J'} = -1 \rangle = 0.12\mu_B$ (the quantity μ_B is the Bohr magneton) for linearly polarized light, which is the polarization that we use in our experiment. This is the first direct measurement of the magnetic-dipole matrix element of an optical transition. From this matrix element, we use Wigner-Eckart theorem to calculate the reduced matrix element of this transition which gives $\langle {}^7F_0 || \mu^{(1)} || {}^5D_1 \rangle = 0.21\mu_B$. This experimentally measured value for the reduced matrix element is in reasonable agreement with the calculations, which predict $\langle {}^7F_0 || \mu^{(1)} || {}^5D_1 \rangle = 0.36\mu_B$. We will not present the details of these calculations here since they are somewhat involved, but we plan to discuss them in detail in a future publication [28].

3 Left-handed waves using induced polarization and magnetization

In this section, we will discuss a new approach for observing left-handed electromagnetic waves and negative refraction. This approach shares a lot of the same physics with negative-index ma-

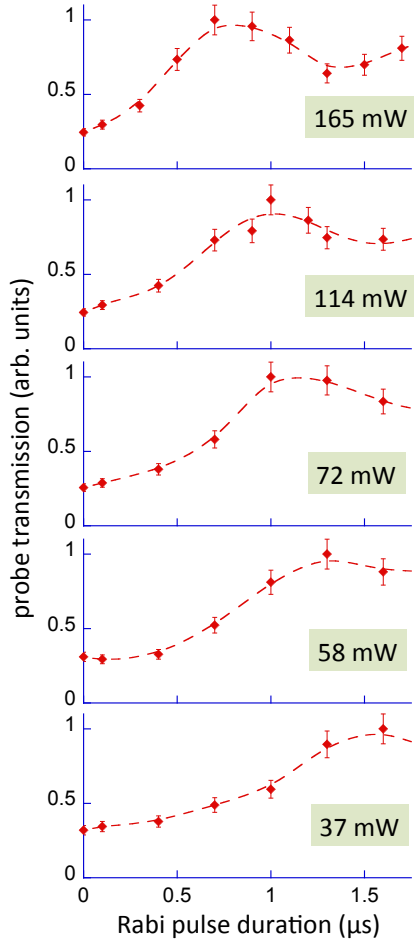


Figure 7: The transmission of the probe laser beam as a function of the duration of the Rabi pulse for different values of the optical power of the Rabi beam. As the beam power is reduced, the Rabi flopping frequency steadily decreases. From each Rabi oscillation curve, we deduce the flopping frequency. These measured frequencies for each beam power is summarized in Fig. 8.

terials (for example these materials exhibit negative refraction), but experimentally is far easier to implement. A detailed description of this idea can be found in our recent publication [27]. Briefly, inside a polarized and magnetized material, the displacement vector \vec{D} and the magnetic field \vec{B} are modified to include the polarization (\vec{P}) and the magnetization (\vec{M}): $\vec{D} = \epsilon_0 \vec{E} + \vec{P}$ and $\vec{B} = \mu_0 \vec{H} + \mu_0 \vec{M}$. The medium can be polarized and magnetized at a specific frequency ω using a number of processes. The most obvious one would be if the frequency of the incident electromagnetic wave is close to an electric-dipole (or a magnetic-dipole) resonance, then the incident wave itself can polarize (or magnetize) the medium through the linear response of the material. It is important to note that the medium can also be polarized or magnetized at a frequency ω using external means (i.e., processes that do not depend on the incident probe wave). The easiest way to understand our idea is to analyze plane wave solutions of Maxwell's equations in the presence of externally induced polarization and magnetization. With the medium externally polarized and magnetized, forced-wave solutions can be found with electric and magnetic field vectors of appropriate magnitude and π out of phase with the induced polarization and magnetization. Under these conditions, there are sign-flips in Maxwell's equations closely mimicking a material with negative permittivity and permeability. The electromagnetic waves of these solutions are left-handed with the vectors \vec{E} , \vec{H} , and \vec{k} forming a left-handed triad.

3.1 Numerical simulations: negative refraction

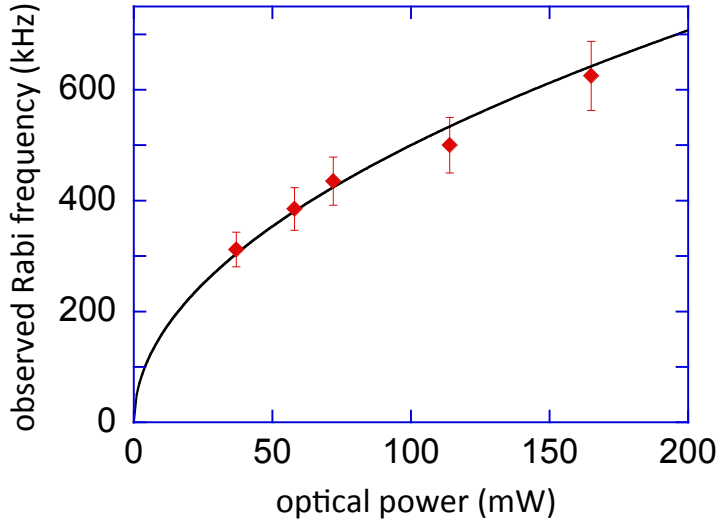


Figure 8: The Rabi flopping frequency as the power of the beam is varied. As the beam power is varied from 165 mW to 37 mW, the Rabi flopping frequency decreases from 625 kHz to 312 kHz, respectively. The solid line shows that the data points fit well to the expected square-root dependence. From this fit we extract the value of the magnetic-dipole matrix element.

To verify our idea, we have performed finite-difference simulations of Maxwell’s equations without any approximations. These simulations have demonstrated robust left-handed wave propagation inside materials with induced polarization and magnetization [27]. We have also investigated refraction at an interface using these simulations which we discuss in this section. Consider an electromagnetic wave refracting from a “normal”, right-handed material (medium 1) to a material with induced polarization and magnetization (medium 2) as shown in Fig. 9(a). From the boundary conditions at the interface, the wave can be shown to refract with a negative angle with the k -vector and the field quantities as shown in Fig. 9(a) [1, 27]. Figure 9(b) shows the time-reversed case where the wave refracts from the EIPM material into free-space.

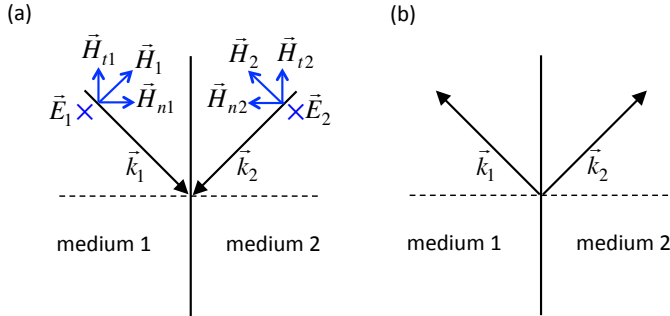


Figure 9: (a) Beam refraction from a “normal”, right-handed material into an EIPM material. Using the boundary conditions at the interface, the wave can be shown to refract with a negative angle. (b) The time-reversed case where the wave refracts from the EIPM material into the right-handed material.

In Fig. 10, we numerically simulate refraction of a wave from the EIPM material into free-space [i.e. for the conditions of Fig. 9(b)]. Here, we assume polarization and magnetization waves in the material (prepared, for example, using the scheme of Fig. 11 that we will discuss below) propagating along the k -vector as shown in Fig. 9(b), away from the interface. We start the numerical integration with zero initial field values, $\vec{H}(x, y, t = 0) = 0$ and $\vec{E}(x, y, t = 0) = 0$. The induced polarization and magnetization generates the left-handed wave in the material, which in turn refracts into free-space. The false-color plots in Fig. 10 show the snapshots for the electric field in the two spatial dimensions, x and y , at $t = 0$, $t = 30$ fs, $t = 60$ fs, and $t = 90$ fs. The boundary between the two regions is at $x = 0$.

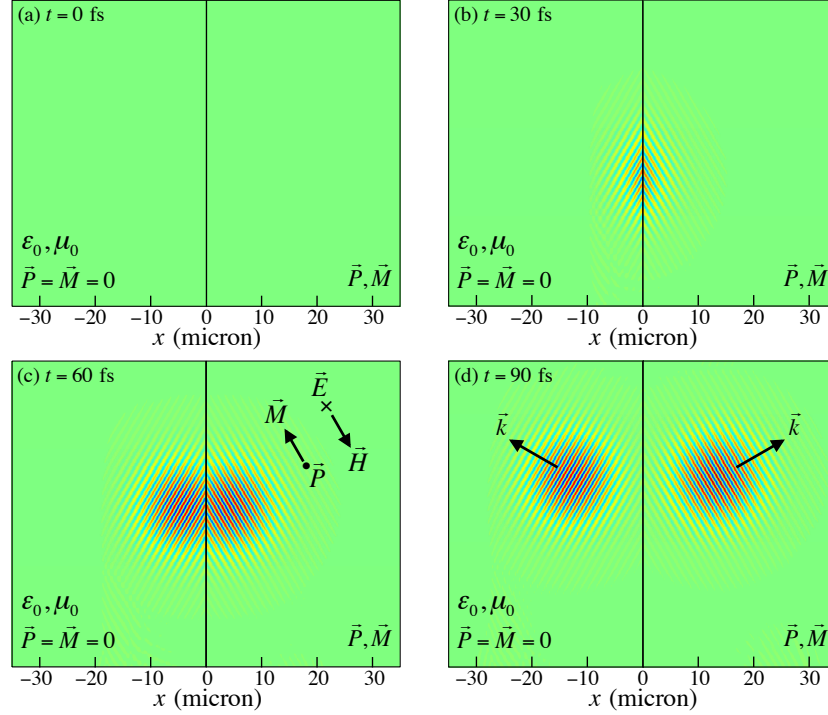


Figure 10: Wave refraction from a material with induced polarization and magnetization into free-space. Before the polarization and magnetization exist in the region on the right, there is no generated EM wave (a). Once the induced polarization and magnetization appear at the interface, a refracted right-handed wave appears in the region of free space (b). As the polarization and magnetization generate the left-handed wave in the region of $x > 0$ a refracted wave is generated along with it in the region of free space. The direction of the polarization, magnetization, electric field, and magnetic field are indicated (c). After the pulse of polarization and magnetization has completely entered the region of $x > 0$ the left-handed wave inside the material and the refracted right-handed wave outside the material propagate as expected (d).

3.2 Proposed scheme for observing left-handed waves in Eu:YSO

Figure 11 shows the scheme that we plan to pursue to excite left-handed waves in Eu:YSO. We plan to magnetize the crystal using the ${}^7F_0 \rightarrow {}^5D_1$ strong magnetic-dipole transition of the Eu^{+3} ions. To generate the coherence between the two levels, we plan to use two-photon excitation with our infrared light at a wavelength of 1054.8 nm. The electric field of this laser beam is referred to as E_ω in Fig. 11. The transitions within the $4f$ shell in a free-ion are dipole forbidden due to parity selection rules (inside the crystal, these transitions become weakly dipole allowed due to the mixing with the crystal field; however this mixing is small). As a result, for two photon excitation, we plan to use the high-lying $4f5d$ configuration as the intermediate level. The goal will be to produce a reasonably large coherence of the magnetic dipole transition, ρ_m , and therefore produce a substantial magnetization at the doubled frequency, $M_{2\omega}$. With the crystal magnetized using the Eu^{+3} ions, we then plan to use the second-order nonlinear response of the host crystal (YSO) to polarize the crystal. Due to the second order susceptibility, $\chi^{(2)}$, a separate infrared field E_ω will produce a nonlinear polarization of magnitude $P_{2\omega} = \epsilon_0 \chi^{(2)} E_\omega^2$.

A quick check of the numbers immediately reveal that, as expected, the key challenge will be to induce a sufficiently large magnetization. To our knowledge, the second order susceptibility of the

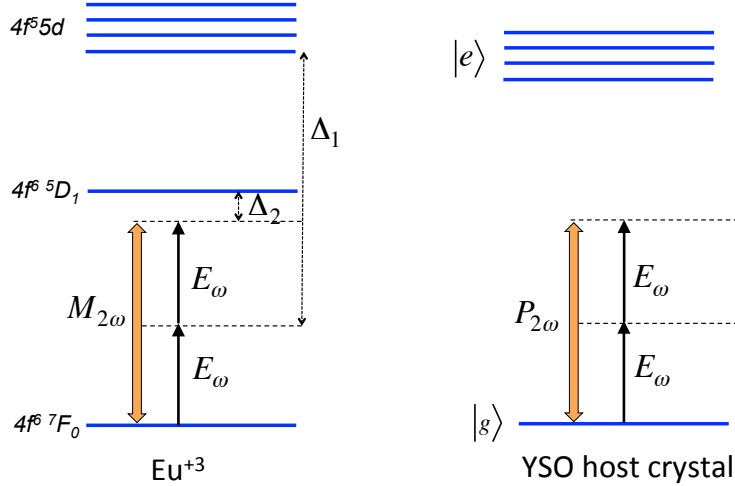


Figure 11: Proposed scheme for exciting left handed waves in a Eu:YSO crystal. The magnetization ($M_{2\omega}$) is induced using the ${}^7F_0 \rightarrow {}^5D_1$ strong magnetic-dipole transition of the Eu^{+3} ions. Two-photon excitation with infrared light at a wavelength of 1054.8 nm (with field amplitude E_ω) is used to generate the coherence between the two levels. The two-photon excitation is through the $4f5d$ configuration as the intermediate level. The polarization is induced using the second-order nonlinear response of the host crystal (YSO). The second order susceptibility ($\chi^{(2)}$) of the YSO crystal produces a nonlinear polarization $P_{2\omega} = \epsilon_0 \chi^{(2)} E_\omega^2$. The beam that induces the polarization is orthogonally polarized to the beam that induces magnetization.

YSO crystal has not yet been measured. However, even if we assume a second order susceptibility which is many orders of magnitude smaller than other common crystals [for example, quartz (SiO_2) and many other crystals have $\chi^{(2)} \approx 10^{-12}$ m/V], we calculate that it is not difficult to induce a sufficiently large polarization in the crystal. Because producing sufficient magnetization is the key challenge, it is important to perform an accurate calculation for the two-photon excitation scheme of the magnetic-dipole transition in Eu^{+3} ions. We have performed this calculation whose details can be found in our publication [27]. Figure 12 shows the calculated intensity of left-handed waves as the focused spot size of the 1054.8 beam is varied (we assume an optical power of 1 W). Even for a reasonably large spot size of 100 μm , it should be possible to excite left-handed waves with easily detectable intensity levels. We are very excited about the calculation of Fig. 12 since this is the first calculation that predicts the formation of left-handed waves in an atomic system using realistic parameters. Once these waves are formed, we plan to study the refraction of these waves as predicted in Fig. 10.

4 Conclusions and outlook

In conclusion, our long-term goal in this project is to demonstrate the first negative refraction in atomic systems. Our key achievements over the last three years have been: (i) We have identified a strong magnetic-dipole transition in europium ions (${}^7F_0 \rightarrow {}^5D_1$ transition), and constructed our experimental system to study this transition in $\text{Eu}^{+3}:\text{Y}_2\text{SiO}_5$. (ii) We performed the first precision spectroscopy, excited state lifetime, and spectral hole burning studies of this transition. (iii) We have observed Rabi flopping of this transition at a rate approaching 1 MHz. As mentioned above, this is the first time Rabi flopping of a magnetic-dipole transition in the optical region has been observed. (iv) We have proposed a new approach for producing left-handed waves and negative refraction in a medium. In these externally polarized and magnetized materials the formation of

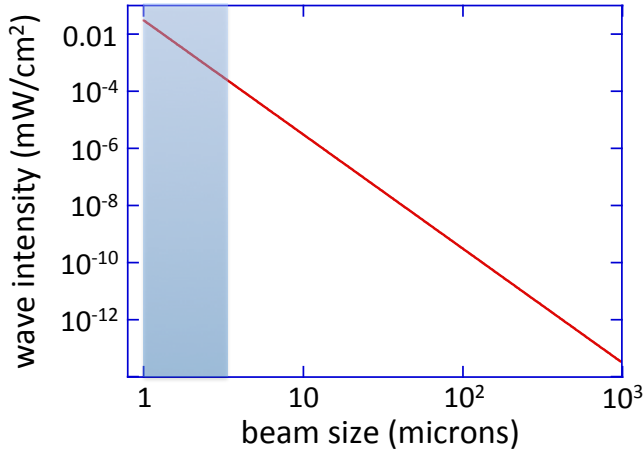


Figure 12: The predicted intensity of the left-handed waves that can be excited inside a 0.1% doped Eu:YSO crystal. Here we take the power of the infrared laser beam ($\lambda = 1054.8$ nm) to be 1 W and calculate the intensity of the left-handed waves as we vary the focused beam size. The shaded region of the curve is speculative since the intensity of the laser becomes sufficiently high that other nonlinear processes can no longer be ignored.

left-handed waves does not require as stringent material properties (compared to negative-index materials). (v) We have evaluated this new scheme in Eu:YSO, and our numerical calculations predict that left-handed electromagnetic waves can be observed inside an Eu:YSO crystal using modest experimental parameters.

We believe this project has already made a significant impact on our understanding of light-matter interactions. We have shown, for the first time, that atoms can interact strongly with the magnetic field of a light wave. This is important since negative refraction studies relies critically on the strength of the magnetic interaction. For the first time, observing negative refraction and left-handed electromagnetic waves in atomic systems seems within reach. As mentioned above, if these effects are observed in atomic systems, we expect a wide range of practical applications such as the construction of lenses with the capability to beat the diffraction limit.

References

- [1] V. G. Veselago, *The Electrodynamics of Substances with Simultaneously Negative Values of ϵ and μ* , Sov. Phys. Usp. **10**, 509 (1968).
- [2] J. B. Pendry, *Negative Refraction Makes a Perfect Lens*, Phys. Rev. Lett. **85**, 3966 (2000).
- [3] D. Schurig, J. J. Mock, B. J. Justice, S. A. Cummer, J. B. Pendry, A. F. Starr, D. R. Smith, *Metamaterial Electromagnetic Cloak at Microwave Frequencies*, Science **314**, 977 (2006).
- [4] J. B. Pendry, A. Aubry, D. R. Smith, and S. A. Maier, *Transformation Optics and Subwavelength Control of Light*, Science **337**, 549 (2012).
- [5] R. A. Shelby, D. R. Smith, and S. Shultz, *Experimental Verification of a Negative Index of Refraction*, Science **292**, 77 (2001).
- [6] A. H. Houck, J. B. Brock, and I. L. Chuang, *Experimental Observations of a Left-Handed Material That Obeys Snells Law*, Phys. Rev. Lett. **90**, 137401 (2003).

- [7] T. J. Yen, W. J. Padilla, N. Fang, D. C. Vier, D. R. Smith, J. B. Pendry, D. N. Basov, and X. Zhang, *Terahertz Magnetic Response from Artificial Materials*, Science **303**, 1494 (2004).
- [8] V. M. Shalaev, W. Cai, U. K. Chettiar, H. Yuan, A. K. Sarychev, V. P. Drachev, and A. V. Kildishev, *Negative Index of Refraction in Optical Metamaterials*, Opt. Lett. **30**, 3356 (2005).
- [9] M. O. Oktel and O. E. Mustecaplioglu, *Electromagnetically Induced Left-Handedness in a Dense Gas of Three-Level Atoms*, Phys. Rev. A **70**, 053806 (2004).
- [10] Q. Thommen and P. Mandel, *Electromagnetically Induced Left Handedness in Optically Excited Four-Level Atomic Media*, Phys. Rev. Lett. **96**, 053601 (2006).
- [11] J. Kästel, M. Fleischhauer, S. F. Yelin, and R. L. Walsworth, *Tunable Negative Refraction without Absorption via Electromagnetically Induced Chirality*, Phys. Rev. Lett. **99**, 073602 (2007).
- [12] D. E. Sikes and D. D. Yavuz, *Negative Refraction with Low Absorption using Raman Transitions with Magneto-Electric Coupling*, Phys. Rev. A **82**, 011806(R) (2010).
- [13] D. E. Sikes and D. D. Yavuz, *Negative Refraction Using Raman Transitions and Chirality*, Phys. Rev. A **84**, 053836 (2011).
- [14] P. P. Orth, R. Hennig, C. H. Keitel, and J. Evers, *Negative Refraction with Tunable Absorption in an Active Dense Gas of Atoms*, N. J. of Physics **15**, 013027 (2013).
- [15] M. O. Scully and M. S. Zubairy, *Quantum Optics* (Cambridge University Press, Cambridge, 1997).
- [16] S. E. Harris, *Electromagnetically Induced Transparency*, Phys. Today **50**, No. 7, 36 (1997).
- [17] R. M. Macfarlane, *High-Resolution Laser Spectroscopy of Rare-Earth Doped Insulators: A Personal Perspective*, J. Lumin. **100**, 1 (2002).
- [18] B. G. Wybourne, *Spectroscopic Properties of Rare-Earths* (John Wiley & Sons, 1965).
- [19] R. M. Macfarlane and R. M. Shelby, *Homogeneous Line Broadening of Optical Transitions of Ions and Molecules in Glasses*, J. Lumin. **36**, 179 (1987).
- [20] B. S. Ham, P. R. Hemmer, and M. S. Shahriar, *Efficient Electromagnetically Induced Transparency in a Rare-earth Doped Crystal*, Opt. Commun. **144**, 227 (1997).
- [21] J. Klein, F. Beil and T. Halfmann, *Rapid Adiabatic Passage in a $Pr^{+3}:Y_2SiO_5$ Crystal*, J. Phys. B: At. Mol. Opt. Phys. **40**, 345 (2007).
- [22] R. W. Equall, Y. Sun, R. L. Cone, and R. M. Macfarlane, *Ultralow Optical Dephasing in $Eu^{+3}:Y_2SiO_5$* , Phys. Rev. Lett. **72**, 2179 (1994).
- [23] B. Lauritzen, N. Timoney, N. Gisin, M. Afzelius, H. de Rietmatten, Y. Sun, R. M. Macfarlane, and R. L. Cone, *Spectroscopic Investigations of $Eu^{+3}:Y_2SiO_5$ for Quantum Memory Applications*, Phys. Rev. B **85**, 115111 (2012).
- [24] M. Kasperczyk, S. Person, D. Ananias, L. D. Carlos, and L. Novotny, *Excitation of Magnetic Dipole Transitions at Optical Frequencies*, Phys. Rev. Lett. **114**, 163903 (2015).

- [25] F. Graf, A. Renn, G. Zumofen, and U. Wild, *Photon-Echo Attenuation by Dynamical Processes in Rare-Earth-Ion-Doped Crystals*, Phys. Rev. B **58**, 5462 (1998).
- [26] R. Yano, M. Mitsunaga, and N. Uesugi, *Ultralong optical dephasing time in Eu:YSO*, Opt. Lett. **16**, 1884 (1991).
- [27] D. D. Yavuz and N. R. Brewer, *Left-Handed Electromagnetic Waves in Materials with Induced Polarization and Magnetization*, Phys. Rev. A, **90**, 063807 (2014).
- [28] N. R. Brewer, Z. Buckholtz, Z. J. Simmons, and D. D. Yavuz (to be published).

1.

1. Report Type

Final Report

Primary Contact E-mail**Contact email if there is a problem with the report.**

yavuz@wisc.edu

Primary Contact Phone Number**Contact phone number if there is a problem with the report**

608-263-9399

Organization / Institution name

University of Wisconsin-Madison

Grant/Contract Title**The full title of the funded effort.**

Negative Refraction in Rare-Earth Doped Crystals

Grant/Contract Number**AFOSR assigned control number. It must begin with "FA9550" or "F49620" or "FA2386".**

FA9550-13-1-0111

Principal Investigator Name**The full name of the principal investigator on the grant or contract.**

Deniz D. Yavuz

Program Manager**The AFOSR Program Manager currently assigned to the award**

Tatjana Curcic

Reporting Period Start Date

03/01/2013

Reporting Period End Date

02/29/2016

Abstract

In this project, our long-term goal is to demonstrate the first negative refraction in atomic systems. Although the concept of negative refraction remained an academic curiosity for a long time, it is now well-understood that negative refraction may have important and far-reaching practical implications. About a decade ago it was discovered that negative index materials can be used to construct devices that can image objects with, in principle, unlimited resolution, i.e., perfect lenses. Currently, many groups around the world are working towards constructing high-quality negative index materials with low absorption. Whereas most groups with this goal rely on meta-materials (artificially constructed structures), we are using atomic systems that are driven with lasers in their internal states.

The key challenge in observing negative refraction in the optical region of the spectrum is the weakness of the magnetic response. Our central experimental result during this project has been the first observation of Rabi flopping of a magnetic-dipole transition in the optical region of the spectrum. We have performed this experiment using the 7F0-5D1 transition of europium ions in a doped yttrium orthosilicate crystal at a temperature of 4 Kelvin. As we will discuss below, we have been able to achieve Rabi flopping frequencies approaching 1 MHz. This is a major result; we have shown for the first time that an electron can interact sufficiently strongly with the magnetic-field of a light wave and move coherently between the two levels (as

DISTRIBUTION A: Distribution approved for public release.

a result of the magnetic interaction). Another important result during this project was the proposal of a new type of materials that exhibit negative refraction. These are materials where the medium is polarized and magnetized externally, i.e., through means other than the incident probe wave (for example, using other lasers and optical nonlinearities). Compared to materials with a negative refractive index, there is one clear advantage of materials with induced polarization and magnetization: the formation of left-handed waves does not require the stringent material properties (such as the strength of the resonances, the density of radiators, and so on).

Distribution Statement

This is block 12 on the SF298 form.

Distribution A - Approved for Public Release

Explanation for Distribution Statement

If this is not approved for public release, please provide a short explanation. E.g., contains proprietary information.

SF298 Form

Please attach your [SF298](#) form. A blank SF298 can be found [here](#). Please do not password protect or secure the PDF. The maximum file size for an SF298 is 50MB.

[SF298_form_final_performance_report.pdf](#)

Upload the Report Document. File must be a PDF. Please do not password protect or secure the PDF. The maximum file size for the Report Document is 50MB.

[Yavuz_2016_AFOSR_Negative_Index_Final_Performance_Report.pdf](#)

Upload a Report Document, if any. The maximum file size for the Report Document is 50MB.

Archival Publications (published) during reporting period:

1] D. D. Yavuz, N. R. Brewer, J. A. Miles, and Z. J. Simmons, Suppression of Inhomogeneous Broadening Using the AC Stark Shift, Phys. Rev. A 88, 063836 (2013).

[2] J. A. Miles, Z. J. Simmons, and D. D. Yavuz, Subwavelength Atom Localization Using Electromagnetically Induced Transparency, Phys. Rev. X 3, 031014 (2013). This paper was selected for a Physics viewpoint: M. Paternostro, Localize and Conquer, Physics 6, 99 (2013).

[3] D. D. Yavuz and N. R. Brewer, Left-handed electromagnetic waves in materials with induced polarization and magnetization, Phys. Rev. A 90, 063807 (2014).

[4] N. R. Brewer, Z. Buckholtz, Z. J. Simmons, and D. D. Yavuz, Rabi Flopping of a Magnetic Dipole Optical Transition (to be submitted to Phys. Rev. Lett).

2. New discoveries, inventions, or patent disclosures:

Do you have any discoveries, inventions, or patent disclosures to report for this period?

No

Please describe and include any notable dates

Do you plan to pursue a claim for personal or organizational intellectual property?

Changes in research objectives (if any):

Change in AFOSR Program Manager, if any:

Extensions granted or milestones slipped, if any:

AFOSR LRIR Number

LRIR Title

Reporting Period

Laboratory Task Manager

Program Officer

Research Objectives**Technical Summary****Funding Summary by Cost Category (by FY, \$K)**

	Starting FY	FY+1	FY+2
Salary			
Equipment/Facilities			
Supplies			
Total			

Report Document**Report Document - Text Analysis****Report Document - Text Analysis****Appendix Documents****2. Thank You****E-mail user**

May 27, 2016 16:34:06 Success: Email Sent to: yavuz@wisc.edu